Solid-State Electronics 200 (2023) 108530

Contents lists available at ScienceDirect

Solid State Electronics

journal homepage: www.elsevier.com/locate/sse

Analysis of 1/f and G–R noise in Phosphorene FETs☆

Adhithan Pon *, M. Ehteshamuddin, Kumar Sheelvardhan, Avirup Dasgupta *

Department of ECE, Indian Institute of Technology Roorkee, Uttarakhand 247667, India

ARTICLE INFO

Keywords:
2D–FET
DFT
Flicker
Phosphorene
Noise

ABSTRACT

This work deals with insights into low-frequency noise in phosphorene FETs. In addition to the flicker noise component, which is often reported in the literature, we also look at generation–recombination (G–R) noise. We evaluate the dependence of noise on the number of layers for both armchair (AC) and zigzag (ZZ) orientations. We also extract the noise parameters for this device.

1. Introduction

Two dimensional Field Effect Transistors (2D–FETs) are being actively investigated for future technology nodes [1]. For efficient use of these devices, understanding the noise behavior is of crucial importance [2]. Noise information also helps us understand the material better. For example, to understand the carrier dynamics in the 2D material systems, low-frequency noise spectroscopy is used as it provides information about trap energy levels and traps concentration values. This insight is highly useful for improving passivation and annealing processes. Noise analysis is equally important for any form of circuit application.

Of the various 2D materials being explored, phosphorene is currently receiving significant attention as it has a combination of useable bandgap and mobility values [3]. Many phosphorene-FET-based experiments have also been reported [4]. However, reports on noise characterizations are quite limited [5], and a better understanding of noise dynamics is required.

In this work, we develop a framework to analyze the low-frequency noise in phosphorene FETs. This work uses first principle based simulations to calculate the material properties including all necessary physical effects while using first-principle calibrated TCAD for FET simulations. We analyze the noise behavior in Phosphorene FETs for multiple layers (N = 1–4) and both the orientations: armchair (AC) and zigzag (ZZ).

2. Computational setup

We employ a semi-classical method to calculate the noise in Phosphorene FETs. The detailed method/flow is presented our previous works [6]. The whole approach is divided into three parts: (a) computation of the electronic properties of single and multilayer Phosphorene using Density Functional Theory (DFT), (b) incorporating the electrical parameters into device simulation using TCAD and (c) noise parameters extraction and analysis.

2.1. Computation of Phosphorene layer electrical parameters

Phosphorene has a puckered honeycomb crystalline symmetric structure. The lattice parameters and orientation are presented in (Fig. 1). We obtained the Phosphorene properties using DFT simulation [7,8].

We used the Meta Generalized Gradient Approximation (MGGA) and TB09LDA functionals which provide accurate results over Local-density approximations (LDA) and GGA due to the inclusion of exact exchange–correlation. For this band structure calculation, we have used 14 × 14 × 1 k-points sampling with 98 irreducible, and the density mesh cut-off was set to 150 Rydberg. The obtained bandgap of monolayer Phosphorene is 1.45 eV which exactly matches with experimental data [9]. The bandgap values of two to four layers (2L–4L) were obtained and found to be in agreement with experimental data [9]. It is found that phosphorene exhibits direct bandgap and there is a dramatic decrease in the bandgap when the number of layers changes from 1L to 3L (Fig. 2) whereas it decreases slightly when the number of layers is increased further. The computed bandgap values and the effective masses of electrons and holes are presented Fig. 2. The obtained effective mass of armchair direction is less than the zigzag.

2.2. Device simulation

Extensive work has been done to create a phosphorene material file for TCAD simulations using the result of the DFT simulations. The

☆ The review of this paper was arranged by Francisco Gamiz.

* Corresponding authors.
E-mail addresses: pon.adhi@gmail.com (A. Pon), avirup@ece.iitr.ac.in (A. Dasgupta).

https://doi.org/10.1016/j.sse.2022.108530

Available online 21 November 2022

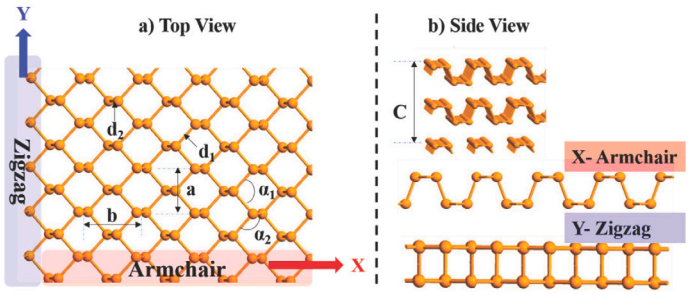

Parameters	Notation	Values
Lattice constant in	a	3.3138
Orthorhombic system	b	4.3759
(Å)	c	10.477
Bond length (Å)	d_1	2.222
	d_2	2.227
Bond angel	α_1	96.34°
	α_2	102.09°

Fig. 1. The crystal structure of Phosphorene is represented and the X-direction (or armchair edge are shown); the Y-direction (zigzag edge are shown). The lattice constants, bond angles, and inter-layer distance are indicated (a) top and (b) side view that parameters values are given in Table form.

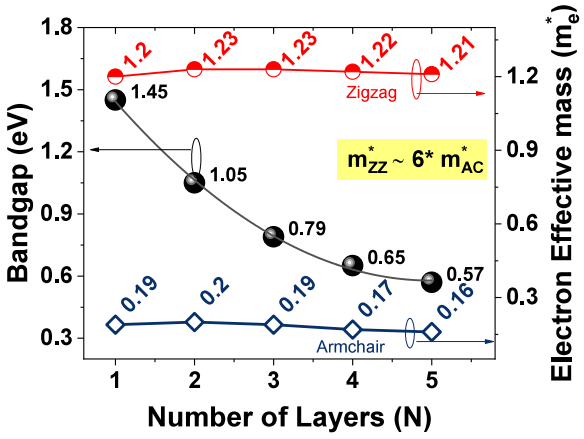

Fig. 2. The phosphorene bandgap and effective mass values are plotted as a function of the number of layers. AC orientation has less effective mass than ZZ. The bandgap is reduced as the number of layers increases due to a reduction in confinement.

quantum effects are included using a 1D schrödinger equation with calibrated ladder parameters. However, Van der Waals interaction and Source/Drain tunneling are not considered.

2.3. Calibration

The drain current calibration was performed considering a dual gate phosphorene MOSFET. We assumed that contacts (Source/Drain) interfaces are perfect and ohmic. We adjusted the Kinetic Velocity Model (KVM) fitting parameters (K_f, α_t, and α_t) and gate metal workfunctions (ϕ_m) to fix a threshold at 100 nA/μm. Appropriate film thickness (t_{si}) and effective oxide thickness (t_{ox}) values were also used to match the drain current with NEGF results (Calibrated parameters are listed in Table 1). Fig. 3 shows the calibration of phosphorene FET against NEGF results [10].

2.4. Noise simulation

To calculate the noise in the phosphorene FET, we use the impedance field method [11]. We consider diffusion, flicker, thermal noise. The noise results are calibrated with experimental data as shown in Fig. 4. From the noise calibration, the extracted Hooge parameter value is $\alpha_h = 5\times10^{-4}$ [5] for bulk phosphorene. The flicker noise ($1/f^{\gamma}$) exponent parameter $\gamma = 1.1$ and the trap density Ntrap = 1×10^{12} cm^{-2}. Layer and orientation-based noise parameters are also calculated while accounting for the thermal noise at high frequencies. In all our noise simulations, we have used an interface trap density of 1×10^{12} cm^{-2}.

Table 1
Material parameters used for simulation.

Parameters	Notation	Values
Affinity	χ	3.9–4.15 eV
Workfunction	ϕ_m	4.2 eV
Doping	N_s and N_d	4×10^{18} cm^{-3}
EOT	t_{ox}	1 nm
Dielectric constant	ϵ_m	14
Lattice Temperature	T	300 K
Film thickness	t_{si}	5–10 nm
Mobility: AC (ZZ)	K_f	15 (20), 0.1 (0.2), 20 (0.3)
	α_t, α_b	0.1 (0.2), 20 (0.3)
Hooge	α_h	$1\times10^{-5} - 5\times10^{-5}$
Trap con.	N_{trap}	1×10^{12} cm^{-2}
DOS	$1L - Nce$	8.42×10^{16} cm^{-2}
	$5L - Nce$	9.77×10^{16} cm^{-2}
	A_e	24.7
Lifetime	τ_0	1×10 μs
Ladder parameters	a,b,c	4.1, 0.7, 23.05

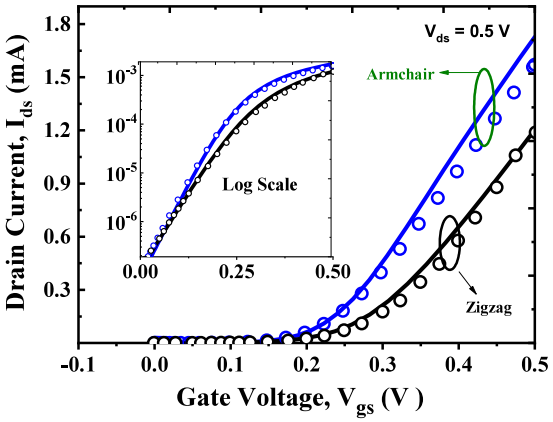

Fig. 3. The calibration of BP-FET against NEGF results [10]. The calibrated parameters are listed in Table 1. Source/drain doped with n-type (4×10^{18} cm^{-3}) and their extension is 14 nm. The contacts are assumed ohmic and trap free.

3. Result and discussion

The noise characteristics of phosphorene FET (N = 1L, AC) is plotted as a function of frequency in Fig. 5. The noise power spectral density (PSD) follows the well-known 1/f behavior. The Generation–Recombination (G–R) noise region is visible at lower frequency [12,13].

There are three main noise components dominant in three different frequency regions. For very low frequencies (10 Hz–1 KHz) G–R noise is dominant due to the (single) trapping and de-trapping of carriers. In the range of 1 KHz–100 MHz, the plot shows clear signs of flicker

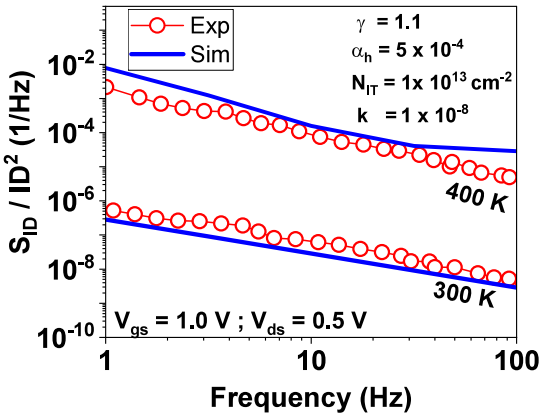

Fig. 4. Noise spectral density (S_{ID}) for bulk phosphorene as a function of frequency and calibrated with [5]. Calibrated noise parameters values are given in the insets. This indicates perfect scaling of $1/f^{\gamma}$ as expected in conventional noise. This trend is affected by the number of layers considered.

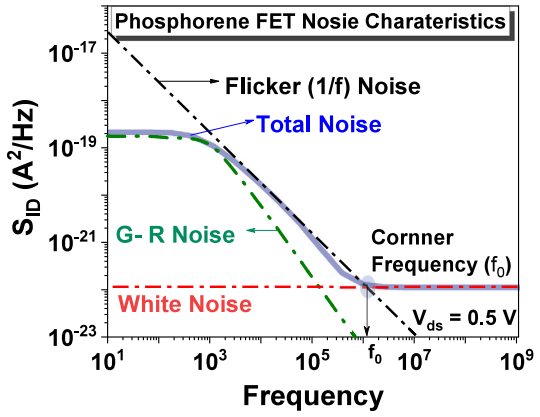

Fig. 5. Noise characteristics of Phosphorene FET (1L-AC). It is found that at low frequencies S_{ID} is high due to a combination of flicker (1/f) and G–R noise. The corner frequency (f_o) is marked, indicating the dominance of the thermal noise floor.

noise (1/f), which is due to carrier and mobility fluctuation in the phosphorene channel. For higher frequencies (greater than f_0 as marked in Fig. 5), the thermal white noise is dominant.

3.1. Layer dependence of extracted γ and K

The general expression for flicker noise power spectral density (S_{ID}) can be given as $S_{ID} = \frac{K}{f^{\gamma}}$, where, $K = W L \alpha_h I_{ds}^2$ while α_h is the Hooge parameter [14], I_{ds} is the drain current of the device while W and L are the width and length of the device, respectively.

Fig. 6. shows the extraction of the flicker noise exponent parameter (γ) at different frequency ranges. We found that γ is frequency dependent for single as well as multi-layer structures. Fig. 6 also shows that gamma is bias dependent, as extracted from S_{ID} for various bias conditions.

Fig. 7 shows the variation of γ and K, with the number of layers as well as for different orientations (AC/ZZ). For ZZ, γ is roughly constant but there is a variation in K for different N, whereas for AC, γ varies while K is a constant.

3.2. Bias dependence of S_{ID}

Fig. 8 shows the gate bias (inset shows the drain bias) dependence of the noise power spectral density (S_{ID}) in phosphorene FETs.

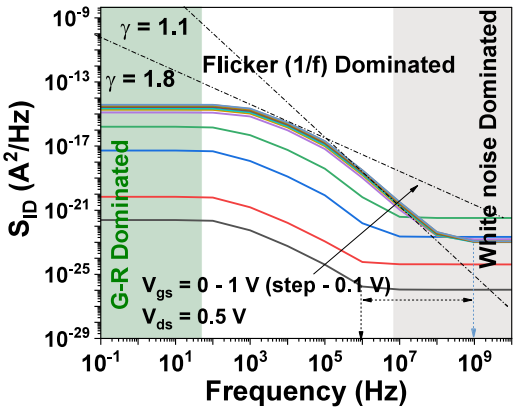

Fig. 6. S_{ID} of phosphorene device (N = 1L AC) as a function of frequency for a range of gate biases Vgs = 0.0 – 1.0 V and Vds = 0.5 V. S_{ID} is saturated after Vgs ≈ 0.4 V due to the onset of strong inversion. γ is also a function of bias.

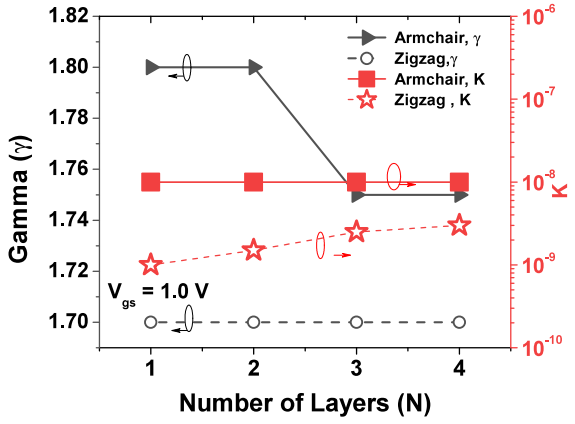

Fig. 7. The gamma (γ) and K values are calculated for different layers. For zigzag orientation γ = 1.7 is constant but K varies with number of layers. For armchair orientation, on the other hand, K is constant but γ varies with number of layers. $S_{ID} = N\ K/(f^{\gamma})$ where, N is number of layers.

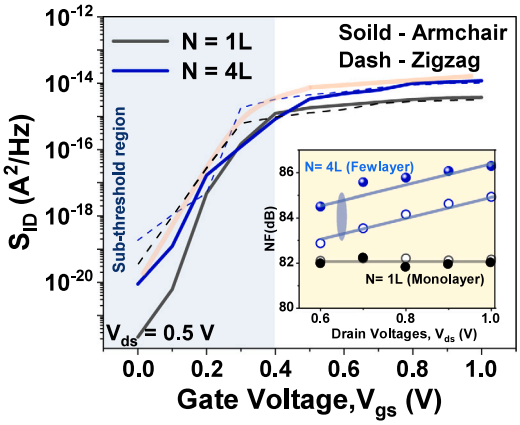

Fig. 8. Noise spectrum plotted as a function of gate and drain bias. It is seen that in the subthreshold region, S_{ID} increases exponentially due to more G–R and diffusion noise. However, drain bias dependence varies with the number of layers. For N = 1L the noise values saturate perfectly due to the very thin nature, whereas for N = 4L it keeps increasing due to more inherent carrier fluctuation than the 1L.

Gate bias: In lower gate bias or in the sub-threshold region (shaded) S_{ID} increases exponentially due to higher carrier fluctuation. S_{ID} saturates at higher V_{gs} for all combinations (1L–4L and AC/ZZ).

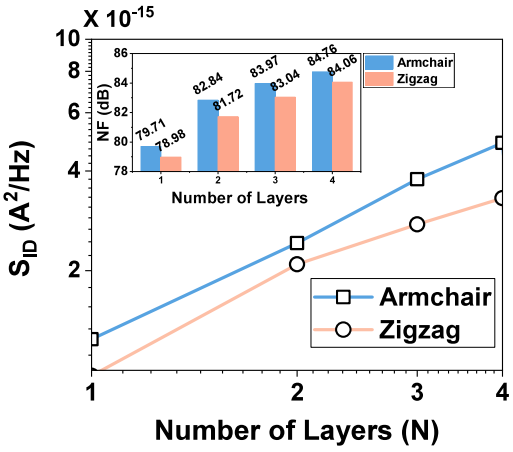

Fig. 9. S_{ID} for phosphorene with different layers. ZZ shows good noise performance over a wide frequency range and for different layer numbers. The inset figure shows the noise figure in the dB for different layers. Since, the noise increases with increasing number of layers.

Drain bias: Inset of Fig. 8 shows that for the monolayer case the noise figure is constant for varying V_{ds} due to the very thin channel, whereas for N = 4L the noise figure increases with V_{ds} due to more inherent carrier fluctuation than the 1L.

3.3. Layer dependence of S_{ID}

Fig. 9 shows that AC has slightly higher noise than ZZ orientation. This is because the higher conductivity for AC results in a higher thermal noise floor. This is true irrespective of the layer number. Due to the addition of volume noise, S_{ID} rises linearly as the layer size grows, while the monolayer case (N = 1L) only contains surface noise. It also shows the Noise Figure (NF in dB) trends in the inset.

4. Conclusion

Through a detailed noise analysis for Phosphorene FETs, we show that for these devices S_{ID} increases with number of layers due to increased charge fluctuation. Also, ZZ has better noise performance than AC for all layer numbers. The Hooge model parameters are also extracted and reported for various combinations. Our analysis suggests that Zigzag monolayer Phosphorene gives the best noise performance for device applications among all possible structures with this material.

Declaration of competing interest

The authors declare that there is no conflict of interest.

Data availability

Data will be made available on request.

Acknowledgments

This work was partially supported by IIT Roorkee, India (FIG/100922) and Science and Engineering Research Board, Govt. of India (SERB/2021/0027).

References

[1] Chhowalla M, Jena D, Zhang H. Two-dimensional semiconductors for transistors. Nat Rev Mater 2016;1(11):1–15.
[2] Balandin AA. Low-frequency 1/f noise in graphene devices. Nature Nanotechnol 2013;8(8):549–55.
[3] Li L, Yu Y, Ye GJ, Ge Q, Ou X, Wu H, et al. Black phosphorus field-effect transistors. Nature Nanotechnol 2014;9(5):372–7.
[4] Yadav S, Jena SR, MB B, Altaee A, Saxena M, Samal AK. Heterostructures of 2D materials-quantum dots (QDs) for optoelectronic devices: challenges and opportunities. Emergent Mater 2021;4(4):901–22.
[5] Liu W, Zheng H, Ang K, Zhang H, Liu H, Han J, et al. Temperature-stable black phosphorus field-effect transistors through effective phonon scattering suppression on atomic layer deposited aluminum nitride. Nanophotonics 2020;9(7):2053–62.
[6] Rathinam R, Pon A, Carmel S, Bhattacharyya A. Analysis of black phosphorus double gate MOSFET using hybrid method for analogue/RF application. IET Circuits Devices Syst 2020;14(8):1167–72.
[7] Smidstrup S, Stradi D, Wellendorff J, Khomyakov PA, Vej-Hansen UG, Lee M-E, et al. First-principles Green's-function method for surface calculations: A pseudopotential localized basis set approach. Phys Rev B 2017;96(19):195309.
[8] Synopsys. Quantumatk O-2018.06. 2018, URL https://www.synopsys.com/silicon/quantumatk.html.
[9] Qiao J, Kong X, Hu Z-X, Yang F, Ji W. High-mobility transport anisotropy and linear dichroism in few-layer black phosphorus. Nature Commun 2014;5(1):1–7.
[10] Cao X, Guo J. Simulation of phosphorene field-effect transistor at the scaling limit. IEEE Trans Electron Devices 2014;62(2):659–65.
[11] Synopsys T. Sentaurus device manual, synopsys sdevice ver. K-2015.06. 2015.
[12] Lin Y-F, Xu Y, Lin C-Y, Suen Y-W, Yamamoto M, Nakaharai S, et al. Origin of noise in layered MoTe2 transistors and its possible use for environmental sensors. Adv Mater 2015;27(42):6612–9.
[13] Sangwan VK, Arnold HN, Jariwala D, Marks TJ, Lauhon LJ, Hersam MC. Low-frequency electronic noise in single-layer MoS2 transistors. Nano Lett 2013;13(9):4351–5.
[14] Hooge FN. 1/f noise is no surface effect. Phys Lett A 1969;29(3):139–40.